

The anti-viral protein of trichosanthin penetrates into human immunodeficiency virus type 1

Wenlong Zhao, Du Feng, Shan Sun, Ting Han, and Senfang Sui*

School of Life Sciences, State Key Laboratory of Biomembrane and Membrane Biotechnology, Tsinghua University, Beijing 100084, China *Correspondence address. Tel: +86-10-62784768; Fax: +86-10-62793367; E-mail: suisf@mail.tsinghua.edu.cn

Trichosanthin (TCS) is a type I ribosome-inactivating protein with potent inhibitory activity against human immunodeficiency virus type 1, and has been clinically applied in acquired immunodeficiency syndrome (AIDS) therapy. Previous studies revealed that TCS recognized human immunodeficiency virus type 1 (HIV-1) particles. Here, we investigated the physical relationship between TCS and HIV-1 particles, and demonstrated that TCS penetrates into viral particles, where it is protected from various protease digestion. The penetration of TCS exerts no obvious effect on viral integrity. FYY140-142, D176, and K177 were identified as key amino acid residues for the membranetranslocation process. Moreover, TCS penetrated into HIV-1 virions showed potent anti-viral activity. Overall, the observations suggest that the penetration of TCS into HIV-1 particles may be important for eliminating the virus.

Keywords trichosanthin; ribosome-inactivating protein; human immunodeficiency virus type 1; virus-like particle; membrane penetration

Received: September 28, 2009 Accepted: November 23, 2009

Introduction

Trichosanthin (TCS) is a type I ribosome-inactivating protein (RIP) extracted from the root tuber of *Trichosanthes kirilowii* [1]. It consists of only a single polypeptide chain, which depurinates A-4324 of mammalian 28S rRNA via an *N*-glycosidase domain, and thus arrests protein synthesis [2]. The protein has multiple functions, including abortifacient, anti-tumor, anti-human immunodeficiency virus (HIV), anti-HSV, and immunoregulatory effects [3]. In the late 1980s, the anti-viral effects of TCS against HIV-1 were described [4,5]. Phase I and II clinical trials were conducted in the USA to evaluate the safety and potential efficacy of this drug. It was shown that TCS elicits a moderate increase in circulating CD4⁺ T cells and a significant decrease of virus load in acquired immunodeficiency syndrome (AIDS) patients failing

treatment with antiretroviral agents such as azidothymidine [6–9]. In addition to TCS, many other RIPs, including *Momordica* anti-HIV protein, pokeweed anti-viral protein, and *Gelonium* anti-HIV protein (GAP31), have been reported to inhibit HIV-1 replication *in vitro* [10].

It was initially thought that TCS inhibits HIV by halting protein translation through RIP activity [11]. However, several mutants with low anti-HIV activity retained their ribosome-inactivating activity [12]. Furthermore, small amounts of TCS specifically inhibit HIV without obvious ribosome inhibiting effects, whereas large amounts induce apoptosis in HIV-1-infected cells [13]. TCS inhibits HIV-1 integrase [14,15], and cleaves supercoiled DNA *in vitro* [16]. It is also associated with and stimulates the activation of chemokine receptors [17].

TCS is a membrane-permeate peptide that is believed to act within the cell and need cross the membrane barrier [3]. TCS interacts with and inserts into artificial phospholipids membrane [18,19]. It induces membrane fusion of liposome [20]. It was also reported that TCS hijacks the cell-derived exosomes for intercellular transport [21]. In our previous report, TCS was shown to recognize HIV-1 with the help of lipid rafts [22]. However, the detailed interaction was elusive. Here, we further studied the physical relationship between TCS and HIV-1, showing that TCS penetrated into viral particles. The penetration had no obvious effect on viral integrity. We also identified important sites for the penetration and revealed that the penetration may be important for virus elimination.

Materials and Methods

Reagents, antibodies, and plasmids

Anti-HIV-1 p24 antibody was purchased from Biodesign International (Saco, USA). Anti-actin antibody was from Santa Cruz Biotechnology (Santa Cruz, USA). Rabbit anti-TCS polyclonal antibody was prepared as standard protocol. Horseradish peroxidase labeled secondary antibody was from Zhongshan Biotechnology (Beijing, China) and gold labeled secondary antibodies were from Jackson

ImmunoResearch (West Grove, USA). The plasmids of Rev-independent Gag were a kind gift from Marilyn D. Resh (Memorial Sloan-Kettering Cancer Center, New York, USA) [23].

Cell culture and transfection

K562 and MT4 cells were maintained in RPMI 1640 (Gibco-BRL, Gaithersburg, USA) supplemented with 10% fetal bovine serum. TZM-bl cells were maintained in DMEM (Gibco-BRL) with 10% fetal bovine serum. Cells were grown to 2×10^7 cells/ml, resuspended in 10 mM HEPES–NaOH-buffered PBS, mixed with 20 μ g plasmids, and further electroporated by BTX ECM 630 electro cell manipulator (Holliston, USA) at 300 V for 20 ms pulse length.

Protein purification and labeling

TCS was extracted from the root tubers of T. kirilowii as described previously [18]. The root tuber obtained from a local drugstore was homogenized with 50 mM Tris-HCl buffer at pH 6.8 (buffer A) using a high-speed blender. The homogenate was centrifuged at 12,000 g for 30 min to remove insoluble material. Then the protein fraction between 40% and 75% ammonium sulfate was collected, precipitated, and dialyzed overnight. The resulting solution was applied to a CM-Sepharose C-50 column (Amersham Biosciences, Buckinghamshire, UK), washed with buffer A, and then eluted with buffer A containing 0.3 M NaCl. The elution peak was collected and loaded onto the second column of Sephadex G-75 (Amersham Biosciences). TCS appeared in the second elution peak. Purity determination of TCS showed a single band of 27 kDa by SDS-PAGE. Fluorescein isothiocyanate (FITC)-labeled TCS was prepared as described [22].

 TCS_{WT} and constructed $TCS_{FYY140-142ASS}$, TCS_{Y55S} , TCS_{K174A} , TCS_{D176A} , TCS_{K177A} were expressed in pGEX-6p-1 plasmids. These proteins were purified by GST Bind Resin according to the manufacturer's protocol (Novagen, Gibbstown, USA). GST tag was removed by PreScission protease (GE Healthcare, Wisconsin, USA).

Preparation of virus-like particles and HIV-1 particles

Virus-like particles (VLPs) were isolated as described previously with some modifications [23]. Briefly, K562 cells were incubated with 0.1 μ M TCS at 24 h post-transfection of HIV-1 Gag. After next 12 h, the culture medium was collected, clarified continuously at 1000 g for 20 min, then 10,000 g for 30 min to remove cell debris, and further filtered through a 0.22- μ M filter (Millipore, Billerica, USA). The filtrate was subjected to ultrafiltration process by 100-kDa MWCO AmiconUltra (Millipore) and washed by extensive PBS to remove free proteins. They were then layered onto the top of a 20% (w/v) sucrose cushion in

PBS and centrifuged for 2 h at 145,000 g (P40ST rotor; Hitachi, Tokyo, Japan). VLPs were recovered from the bottom of the tube. For preparation of HIV-1 particles, MT4 cells (5×10^4 cells/ml) were infected with HIV-1 $_{\rm IIIB}$ stock at a multiplicity of infection (MOI) of 0.015. After 3 days, 0.1 μ M of TCS was incubated for 24 h. Then the medium was collected and the TCS-enriched viruses were purified as VLPs did. The quantity of virus was determined by HIV-1 p24 antigen ELISA kit (Vironostika, Boxtel, The Netherlands) according to the manufacturer's protocol.

Sucrose density gradient centrifugation

After VLPs and TCS-enriched VLPs were filtered through a 20%-sucrose cushion, they were resuspended in 200 μ l PBS and centrifuged at 200,000 g for 16 h in 20–60% linear sucrose equilibrium gradient as described to monitor the viral integrity [24].

Protease protection experiment

VLPs (10 μ l) were incubated with trypsin protease at 0, 1, 3, or 10 μ g in the presence or absence of 0.1% Triton X-100 for 0.5 h at 37°C. The digestion was stopped by 1× protease inhibitor cocktail (Calbiochem, San Diego, USA) and analyzed by western blotting. For subtilisin treatment, VLPs or microvesicles were gently resuspended in TE buffer (20 mM Tris–HCl, pH 8.0, and 2 mM EDTA) [25]. Subtilisin (1 mg/ml) (Fluka, Milwaukee, USA) was used to treat the samples at 37°C for 16 h. The digestion was stopped by 5 μ g/ml phenylmethylsulphonyl fluoride (PMSF; Amresco, Solon, USA), and then pelleted by an ultracentrifugation of 120,000 g for 2 h. The pellets were analyzed by SDS-PAGE and western blotting.

Monolayer study

Monolayer surface pressure was measured using the Wilhelmy plate method with a NIMA 9000 microbalance. Surface pressure (π) was defined as the surface tension difference before and after depositing the monolayer on the solution surface. The sample trough had a volume of 4 ml and a surface area of 10 cm². The sub-phase was stirred continuously with a magnetic bar. In the experiment, mixed phospholipids (PC:PE:cholesterol:sphingomyelin = 0.7:0.7:2.2:1, in molar ratio, plus 1% ganglioside in weight%) were dissolved in chloroform-methanol mixture (3:1; v/v) at a concentration of 1.0 mg/ml and coated onto the buffer surface to form a lipid monolayer. After stabilization of the surface pressure at a designated value, which was considered as initial surface pressure (π_i), the solution of wild-type and mutant TCS in PBS at 0.2 µM was injected into the sub-phase through a side sample hole. The pressure change was monitored until the surface pressure increase $(\Delta \pi)$ had reached a maximum value (usually within 2 h). All the experiments were carried out under N_2 to prevent oxidation of the samples. The temperature of the system was maintained at $25 \pm 0.2^{\circ}$ C. $\Delta \pi$ can be obtained at various π_i values for each sample. The plot of $\Delta \pi$ versus π_i then yields a straight line with negative slope intersecting the abscissa at a limiting surface pressure. The limiting surface pressure, defined as critical insertion pressure (π_c) of the protein sample for corresponding lipid monolayer, was used for quantitative evaluation of the insertion ability of the protein in the phospholipids monolayer.

Bioassays for anti-HIV-1 activity

HIV-1 infectivity was measured by the multinuclearactivation galactosidase indicator (MAGI) assay [26]. In the MAGI assay, 10⁵ cells/ml of TZM-bl cells were infected by equal amounts of HIV-1 or TCS-enriched HIV-1 (normalized for p24, MOI of TCS-free virus was 0.02). Two days post-infection, cells were fixed with 1% formaldehyde and 0.2% glutaraldehyde in PBS. After extensive wash with PBS, cells were stained with a solution of 4 mM potassium ferrocyanide, 4 mM potassium ferrocyanide, 2 mM MgCl₂, and 0.4 mg/ml X-gal. The number of blue cells is measured as viral infectivity.

Results

TCS penetrates into viral particles

For studies of physical relationship between TCS and viral particles, we used plasmids expressing the Revindependent HIV-1 Gag scaffold protein, which is sufficient to produce VLPs. It faithfully mimics the viral budding process and possesses viral envelope [27]. When

cells expressing the HIV-1 Gag were incubated with TCS, the produced TCS-enriched VLPs were collected [Fig. 1(A)] [22]. In order to examine whether TCS penetrates into viral particles, the purified TCS-enriched VLPs were subjected to protease protection experiments. Trypsin alone did not degrade the TCS that was carried by VLPs [Fig. 1(A)]. Increasing concentrations of trypsin protease were also unable to remove all the TCS in VLPs unless the treatment with 0.1% Triton X-100 to permeate the membrane. As a control, the free TCS was completely digested by trypsin [Fig. 1(B)].

Microvesicles as the possible contaminants are usually co-purified with VLPs. It is possible that the cell-derived microvesicles protect TCS from trypsin digestion [21]. Subtilisin degradation method was used to remove proteins on the exterior of virions and eliminated nearly all of contaminating microvesicles in virion samples [Fig. 1(C)] [25]. When exposed to subtilisin alone, only a small portion of TCS and Gag was digested. After treated with Triton X-100 to permeate the membrane, TCS and Gag were completely removed [Fig. 1(D)]. The digestion experiments by two different proteases indicate that at least some of the TCS molecules are penetrating deep into VLPs.

In addition to VLPs, we further examined the distribution of TCS molecules in individual *bona fide* HIV-1 virions. Viruses are normally produced in the TCS-treated cells [Fig. 2(A)]. Immuno-labeling results revealed that most of TCS resided at or near viral membrane, and still some localized deep into the viral lumen [Fig. 2(B,C), arrows]. Thus, TCS is able to penetrate viral envelope and reach the viral lumen.

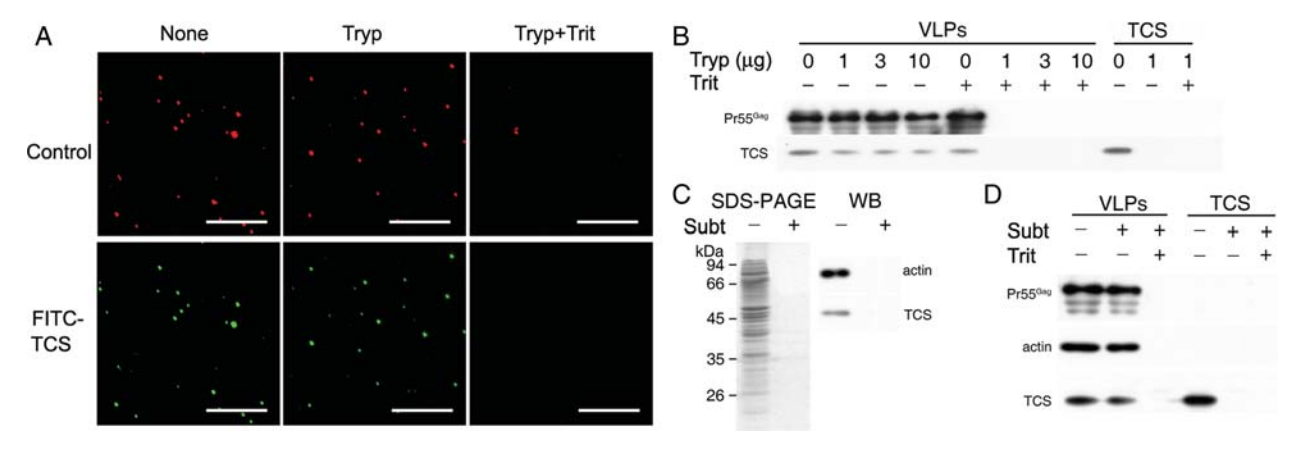


Figure 1 Virion-carried TCS is protected from trypsin and subtilisin digestion (A) FITC-TCS-enriched VLPs (Gag-CFP) were purified and treated by 0.2 mg/ml trypsin for 0.5 h at 37°C alone or with 0.1% Triton X-100. The treated VLPs were loaded onto coverslips and observed by Nikon E800 microscope with fluorescent attachment. Scale bar = 10 μm. (B) TCS-enriched VLPs (10 μl) were treated with various amounts of trypsin in the absence or presence of 0.1% Triton X-100 for 0.5 h at 37°C. Free TCS (2 ng) was also subjected to trypsinization as a control. (C) SDS-PAGE and western blotting (WB) analysis of subtilisin-treated microvesicles. The microvesicles were collected from a large volume of culture medium of TCS-treated K562 cells by 120,000 g ultracentrifugation. Lanes containing non-subtilisin-treated and subtilisin-treated samples were denoted by minus and plus signs, respectively. (D) TCS-enriched VLPs were treated with 1 mg/ml subtilisin in the absence or presence of 0.1% Triton X-100 for 16 h at 37°C. The treated samples were analyzed via western blotting by antibodies for Pr55^{Gag}, actin, and TCS. TCS, trichosanthin, Tryp, trypsin; Trit, Triton X-100; Subt, subtilisin.

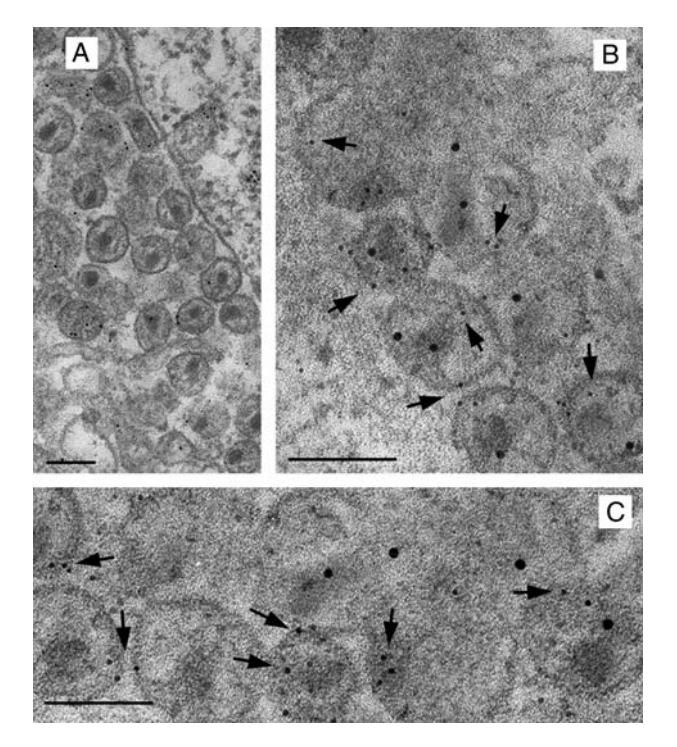


Figure 2 Immuno-electron microscopy analysis of TCS-incubated HIV-1 (A) MT4 cells producing nascent HIV-1 virions were incubated with 0.1 μ M TCS for 2 h and then processed for electron microscopy. (B,C) TCS localization in individual HIV-1 particles was detected by immuno-electron microscopy. HIV-1 p24 (12-nm gold) and TCS (6-nm gold, arrow) are double labeled. Scale bar =100 nm.

TCS penetration exerts no obvious effect on viral integrity

TCS has a strong tendency to associate with and penetrate viral envelope. Such an anti-viral peptide might destabilize the viral membrane and disrupt the viral particles. We used a virus sedimentation assay to determine the impact of TCS on structural integrity of viral particles as described [24]. The buoyant densities of VLPs were compared on a 20–60% sucrose density gradient centrifugation. As shown in **Fig. 3**, TCS-treated and those untreated VLPs sedimented in almost the same density fractions, suggestive of no destabilization effect of TCS. Moreover, in *bona fide* HIV-1, most of TCS-treated virions were in round normal appearance, and held an intact dark core [**Fig. 2(A)**]. Together with the above results that TCS-enriched VLPs

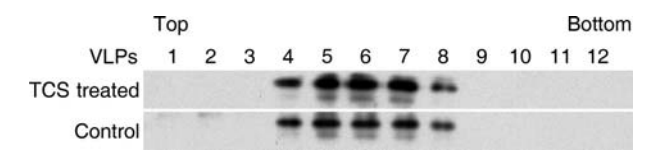


Figure 3 The examination of viral integrity by buoyant sucrose density TCS-enriched or control VLPs were layered onto 20-60% linear sucrose gradient accelerated to equilibrium (16 h at 200,000~g) to monitor particle density. Twelve fractions were collected from the top to the bottom and sequentially analyzed via western blotting by antibody for $Pr55^{Gag}$ to examine the integrity of VLPs.

were largely resistant to protease digestion, these data support that the penetration of TCS seems fail to destabilize the viral envelope and lead to rare aberrant virions.

FYY140-142, D176, and K177 are important for TCS penetrating into VLPs

Since helical hairpin was reported to be critical for membrane translocation of toxins [28], we mutated several amino acids at the loop linker between surface α helixes. Monolayer experiment was carried out to study the insertion ability of TCS into phospholipids [Fig. 4(A)]. Since Demel et al. [29] established that agents known for interacting only with the phospholipids headgroup did not induce a surface-pressure increase in a monolayer, the surface-pressure increases of lipid monolayers after injection of proteins into the sub-phase are only interpreted as the result of actual insertion of the proteins into the phospholipids monolayer. Compared with TCS_{WT}, $TCS_{FYY140-142ASS}$, TCS_{D176A} , and TCS_{K177A} mutants had much lowered critical insertion pressure, indicative of the reduced membrane-insertion ability [Fig. 4(B) Table 1]. We further tested the penetration defects mutants by trypsin digestion. As in Fig. 4(C,D), these mutants had almost the same association ability with VLPs, whereas much lowered penetration capacity, for more peptides could be degraded by the protease. These results indicate that FYY140-142, D176, and K177 are important amino acids for the membrane translocation of TCS into VLPs.

The penetration of TCS may be important for its anti-viral activity

TCS in virions may invade infected cytosol upon viral infection. We thus examined the anti-viral activity of TCS in virion by MAGI assay [26]. Equal amounts of HIV-1 were used for infecting fresh TZM-bl cells. The virion-carried TCS showed highly inhibitory effect on HIV-1 replication when compared with free TCS (**Fig. 5**) [22]. As TCS_{FYY140-142} lost much of the membrane-permeate ability into virions, we then evaluated the anti-viral activity of virions-carried TCS_{FYY140-142}. It was shown that TCS_{FYY140-142} exerts significantly less effect than TCS_{WT} (**Fig. 5**). As the mutant has the same association but reduced penetration ability, we deduce that the penetrated TCS molecules may be important for the anti-viral activity.

Discussion

TCS is an anti-viral peptide that was clinically applied in AIDS therapy [6–9]. We studied the physical relationship between TCS and HIV-1 and described the membrane translocation of TCS into HIV-1 virions. Different from ricin toxin that crosses cell membrane through Sec61 protein pore in ER, TCS itself displays direct membrane

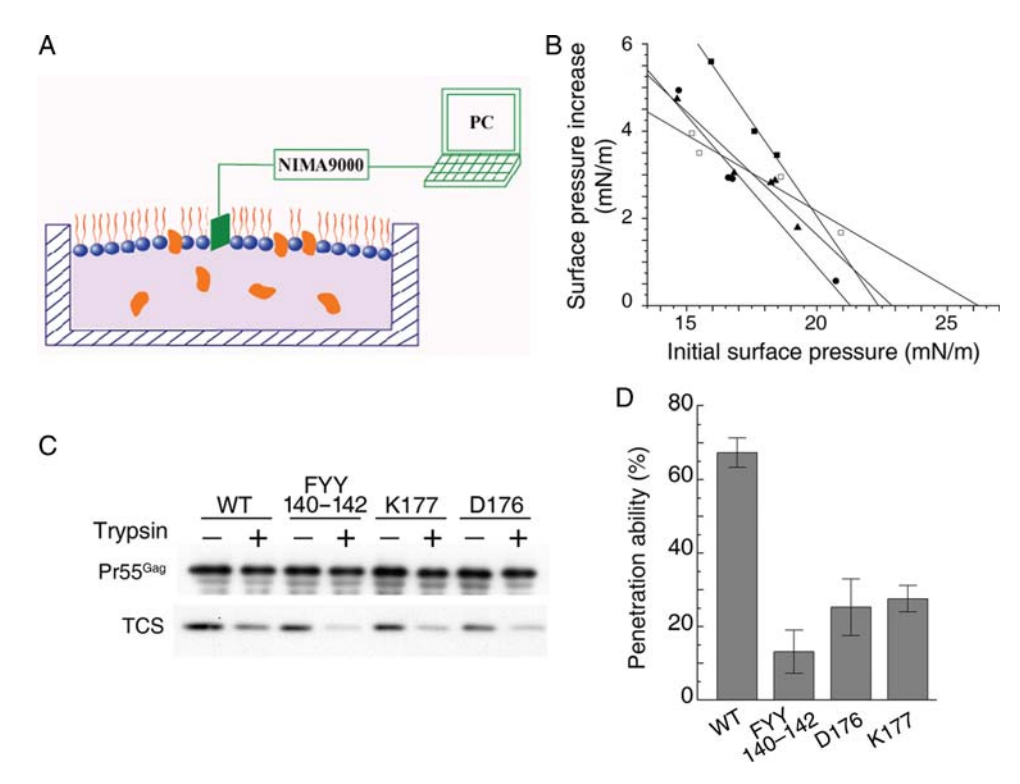


Figure 4 Mutation of FYY140–142, D176 or K177 reduces TCS penetration into VLPs (A) The principle of phospholipids monolayer study. (B) Membrane insertion $\Delta\pi$ (surface pressure increase) versus π (initial surface pressure) curves for TCS_{WT} (open rectangles, R=0.93), TCS_{FYY140–142ASS} (closed triangles, R=0.95), TCS_{D176A} (closed circles, R=0.97) and TCS_{K177A} (closed squares, R=0.99). The final concentration of TCS was 0.2 μ M. The composition of the phospholipids monolayer mimics the viral membrane. The critical insertion pressure is defined as the dot that straight line with negative slope intersects the abscissa, which evaluates the membrane insertion ability of TCS. (C) Membrane-penetration ability of TCS mutants into VLPs. K562 cells producing VLPs were incubated with 0.1 μ M wild-type (WT) or TCS mutants for 2 h. The collected VLPs were divided into two equal fractions, which were then treated by trypsin digestion or not. Western blotting analysis of Pr55^{Gag} and TCS from trypsin-treated VLPs (penetration fraction) and mock-treated VLPs (association fraction) was performed for the membrane translocation study. (D) FITC-TCS was used for quantitative analysis instead of the above TCS. Trypsin-treated and mock-treated VLPs were pelleted and the quantities were measured by fluorescence spectrophotometer (at 495-nm excitation). The penetration efficiency (%) was calculated as the amount of penetrated TCS divided by the amount of associated TCS (mean \pm SEM; n=3).

Table 1 Critical insertion pressure (π_c) of wild-type (WT) and mutated TCS on phospholipid monolayers

WT	Y55S	R174A	FYY140-142ASS	D176A	K177A
26.2	26.1	25.2	22.9	21.3	22.4

penetration ability [3,18,30]. TCS preferentially penetrates at the lipid raft membranes [21], and meanwhile HIV-1 envelope is highly rich in raft regions [31]. Thus, it is conceivable that TCS preferentially penetrates the viral membrane. TCS does not directly disrupt viral particles; on the contrary, TCS in virions may invade infected cytosol to inhibit the viral integration process upon viral infection [15].

The trans-membrane mechanism of TCS is largely elusive. Although previous studies reported several TCS mutants, only the one with seven residues at its C-terminus deleted was shown reduced membrane insertion ability [11,12,20]. The C-terminal deletion mutant also exerted reduced virus-inhibitory activity [12]. It is the first time to identify point mutants that lack membrane penetration

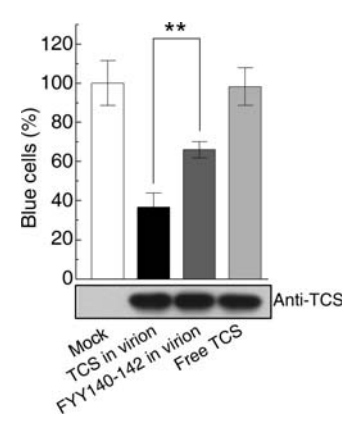


Figure 5 Penetration mutant of TCS shows significantly reduced anti-viral activity The anti-viral activity of TCS in HIV-1 virions was evaluated by MAGI assay. Equal amounts of normal HIV-1, TCS_{WT} -enriched HIV-1, $TCS_{FYY140-142ASS}$ -enriched HIV-1 or HIV-1 with indicated free TCS (\sim 3 ng for 10^5 cells) were used for infecting TZM-bl cells. Two days post-infection, the cells were stained by X-gal. The values indicate percentages of blue cell number compared with that of the control virus (mean \pm SEM; n=3). TCS used in each viral fraction was analyzed by western blotting. The data were analyzed using Student's t-test. **P< 0.01.

ability. The charged amino acids as D176 and K177 are located at the long hairpin loop that extended away from TCS, which may be important for TCS to interact with lipid membrane. The mutation of FYY140–142 to ASS that get rid of only the hydrophobic phenyl group hints the tip of hydrophobic amino acids may be used for insertion into hydrophobic membrane environment.

On viral infection, the so-called 'Trojan exosome hypothesis' was proposed, in which the preexisting nonviral exosome biogenesis pathway is used by retrovirus to form infectious particles [32]. Exosomes are secreted organelles that have the same topology as the cell and bud outward from endosomal membranes. HIV-1 particles and exosomes exhibit many morphological and biochemical similarities, in that both bud from specific areas rich in lipid raft and mediate proteins for intercellular transport [33,34]. Therefore, it is reasonable to assume that TCS is able to penetrate into both HIV-1 and exosomes. Our recent publication supports this notion [21]. TCS is unique in that it shows both anti-tumor and anti-HIV effects, although previous investigations were unable to explain the phenomenon. Because exosomes are actively released by many tumors [35], TCS may hijack tumor cells by way of tumor-derived exosomes [21]. In this study, the penetration of TCS into HIV-1 may contribute to its virus-inhibitory activity. Although the exact intracellular targets may differ, those two pathways are very similar in nature.

Although we elucidated powerful anti-viral activity of the TCS within virions, free TCS is certainly able to inhibit HIV-1 replication. However, the anti-viral effect of only trace amount of free TCS is not so prominent. Under our conditions, only about 3 ng-free TCS was applied to 10⁵ MT4 cells. On the contrary, the same amount of trace TCS in virus-carrying state significantly reduced the HIV-1 infectivity.

In summary, the study provides evidence that the antiviral peptide of TCS penetrates into HIV-1 particles and the penetration may be important for its anti-viral activity. The penetration behavior of TCS into virions may provide implications for design protein-based drug for AIDS therapy.

Acknowledgements

We thank Dr Jingyun Li for the help of HIV-1 work in Laboratory Biosafety Level-3 (Academy of Military Medical Sciences of China, Beijing, China) and Marilyn D. Resh (Memorial Sloan-Kettering Cancer Center, New York, USA) for Gag-GFP plasmid.

Funding

This work was supported by the grants from the National Natural Science Foundation of China (30670501) and National Basic Research Program of China (2010CD833706).

References

- 1 Maraganore JM, Joseph M and Bailey MC. Purification and characterization of trichosanthin. Homology to the ricin A chain and implications as to mechanism of abortifacient activity. J Biol Chem 1987, 262: 11628-11633.
- 2 Zhang JS and Liu WY. The mechanism of action of trichosanthin on eukaryotic ribosomes—RNA N-glycosidase activity of the cytotoxin. Nucleic Acids Res 1992, 20: 1271–1275.
- 3 Shaw PC, Lee KM and Wong KB. Recent advances in trichosanthin, a ribosome-inactivating protein with multiple pharmacological properties. Toxicon 2005, 45: 683–689.
- 4 McGrath MS, Hwang KM, Caldwell SE, Gaston I, Luk KC, Wu P and Ng VL, et al. GLQ223: an inhibitor of human immunodeficiency virus replication in acutely and chronically infected cells of lymphocyte and mononuclear phagocyte lineage. Proc Natl Acad Sci USA 1989, 86: 2844–2848.
- 5 McGrath MS, Santulli S and Gaston I. Effects of GLQ223 on HIV replication in human monocyte/macrophages chronically infected in vitro with HIV. AIDS Res Hum Retroviruses 1990, 6: 1039–1043.
- 6 Kahn JO, Gorelick KJ, Gatti G, Arri CJ, Lifson JD, Gambertoglio JG and Bostrom A, et al. Safety, activity, and pharmacokinetics of GLQ223 in patients with AIDS and AIDS-related complex. Antimicrob Agents Chemother 1994, 38: 260–267.
- 7 Kahn JO, Kaplan LD, Gambertoglio JG, Bredesen D, Arri CJ, Turin L and Kibort T, et al. The safety and pharmacokinetics of GLQ223 in subjects with AIDS and AIDS-related complex: a phase I study. AIDS 1990, 4: 1197–1204.
- 8 Byers VS, Levin AS, Malvino A, Waites L, Robins RA and Baldwin RW. A phase II study of effect of addition of trichosanthin to zidovudine in patients with HIV disease and failing antiretroviral agents. AIDS Res Hum Retroviruses 1994, 10: 413–420.
- 9 Byers VS, Levin AS, Waites LA, Starrett BA, Mayer RA, Clegg JA and Price MR, et al. A phase I/II study of trichosanthin treatment of HIV disease. AIDS 1990, 4: 1189–1196.
- 10 Parikh BA and Tumer NE. Antiviral activity of ribosome inactivating proteins in medicine. Mini Rev Med Chem 2004, 4: 523-543.
- 11 Wang JH, Nie HL, Tam SC, Huang H and Zheng YT. Anti-HIV-1 property of trichosanthin correlates with its ribosome inactivating activity. FEBS Lett 2002, 531: 295–298.
- 12 Wang JH, Nie HL, Huang H, Tam SC and Zheng YT. Independency of anti-HIV-1 activity from ribosome-inactivating activity of trichosanthin. Biochem Biophys Res Commun 2003, 302: 89–94.
- 13 Wang YY, Ouyang DY, Huang H, Chan H, Tam SC and Zheng YT. Enhanced apoptotic action of trichosanthin in HIV-1 infected cells. Biochem Biophys Res Commun 2005, 331: 1075–1080.
- 14 Au TK, Collins RA, Lam TL, Ng TB, Fong WP and Wan DC. The plant ribosome inactivating proteins luffin and saporin are potent inhibitors of HIV-1 integrase. FEBS Lett 2000, 471: 169–172.
- 15 Zhao WL, Feng D, Wu J and Sui SF. Trichosanthin inhibits integration of human immunodeficiency virus type 1 through depurinating the longterminal repeats. Mol Biol Rep 2009, doi: 10.1007/s11033-009-9668-2.
- 16 Li MX, Yeung HW, Pan LP and Chan SI. Trichosanthin, a potent HIV-1 inhibitor, can cleave supercoiled DNA in vitro. Nucleic Acids Res 1991, 19: 6309-6312.
- 17 Zhao J, Ben LH, Wu YL, Hu W, Ling K, Xin SM and Nie HL, et al. Anti-HIV agent trichosanthin enhances the capabilities of chemokines to stimulate chemotaxis and G protein activation, and this is mediated through interaction of trichosanthin and chemokine receptors. J Exp Med 1999, 190: 101–111.
- 18 Xia XF and Sui SF. The membrane insertion of trichosanthin is membrane-surface-pH dependent. Biochem J 2000, 349: 835–841.

- 19 Lu Y, Xia X and Sui SF. The interaction of trichosanthin with supported phospholipid membranes studied by surface plasmon resonance. Biochim Biophys Acta 2001, 1512: 308–316.
- 20 Xia XF, Zhang F, Shaw PC and Sui SF. Trichosanthin induces leakage and membrane fusion of liposome. IUBMB Life 2003, 55: 681-687.
- 21 Zhang F, Sun S, Feng D, Zhao WL and Sui SF. A novel strategy for the invasive toxin: hijacking exosome-mediated intercellular trafficking. Traffic 2009, 10: 411–424.
- 22 Zhao WL, Zhang F, Feng D, Wu J, Chen S and Sui SF. A novel sorting strategy of trichosanthin for hijacking human immunodeficiency virus type 1. Biochem Biophys Res Commun 2009, 384: 347–351.
- 23 Lindwasser OW and Resh MD. Multimerization of human immunodeficiency virus type 1 Gag promotes its localization to barges, raft-like membrane microdomains. J Virol 2001, 75: 7913–7924.
- 24 Bobardt MD, Cheng G, de Witte L, Selvarajah S, Chatterji U, Sanders-Beer BE and Geijtenbeek TB, et al. Hepatitis C virus NS5A anchor peptide disrupts human immunodeficiency virus. Proc Natl Acad Sci USA 2008, 105: 5525–5530.
- 25 Ott DE. Purification of HIV-1 virions by subtilisin digestion or CD45 immunoaffinity depletion for biochemical studies. Methods Mol Biol 2009, 485: 15–25.
- 26 Kimpton J and Emerman M. Detection of replication-competent and pseudotyped human immunodeficiency virus with a sensitive cell line on the basis of activation of an integrated beta-galactosidase gene. J Virol 1992, 66: 2232–2239.

- 27 Morita E and Sundquist WI. Retrovirus budding. Annu Rev Cell Dev Biol 2004, 20: 395–425.
- 28 Silverman JA, Mindell JA, Finkelstein A, Shen WH and Collier RJ. Mutational analysis of the helical hairpin region of diphtheria toxin transmembrane domain. J Biol Chem 1994, 269: 22524–22532.
- 29 Demel RA, London Y, Geurts van Kessel WS, Vossenberg FG and van Deenen LL. The specific interaction of myelin basic protein with lipids at the air-water interface. Biochim Biophys Acta 1973, 311: 507–519.
- 30 Sandvig K and van Deurs B. Membrane traffic exploited by protein toxins.

 Annu Rev Cell Dev Biol 2002, 18: 1–24.
- 31 Brugger B, Glass B, Haberkant P, Leibrecht I, Wieland FT and Krausslich HG. The HIV lipidome: a raft with an unusual composition. Proc Natl Acad Sci USA 2006, 103: 2641–2646.
- 32 Gould SJ, Booth AM and Hildreth JE. The Trojan exosome hypothesis. Proc Natl Acad Sci USA 2003, 100: 10592–10597.
- 33 Booth AM, Fang Y, Fallon JK, Yang JM, Hildreth JE and Gould SJ. Exosomes and HIV Gag bud from endosome-like domains of the T cell plasma membrane. J Cell Biol 2006, 172: 923–935.
- 34 Nguyen DG, Booth A, Gould SJ and Hildreth JE. Evidence that HIV budding in primary macrophages occurs through the exosome release pathway. J Biol Chem 2003, 278: 52347–52354.
- 35 Iero M, Valenti R, Huber V, Filipazzi P, Parmiani G, Fais S and Rivoltini L. Tumour-released exosomes and their implications in cancer immunity. Cell Death Differ 2008, 15: 80–88.